BNL-66691

A DESCRIPTION OF THE GLOBAL SULFUR CYCLE AND ITS CONTROLLING PROCESSES IN THE NCAR CCM3

P. J. Rasch, M. C. Barth, J. T. Kiehl, S. E. Schwartz, and C. M. Benkovitz

July 1999

Accepted for publication in
Journal of Geophysical Research

By acceptance of this article, the publisher and/or recipient acknowledges the U.S. Government's right to retain a nonexclusive, royalty-free license in and to any copyright covering this paper.

Research by BNL authors was performed under the auspices of the U.S. Department of Energy under Contract No. DE-AC02-98CH10886.

A Description of the global sulfur cycle and its controlling processes in the NCAR CCM3

Philip J. Rasch, Mary C. Barth, Jeffrey T. Kiehl

National Center for Atmospheric Research, Boulder, Colorado [1]

Stephen E. Schwartz, Carmen M. Benkovitz

Brookhaven National Laboratory, Upton, New York

Accepted July 1999, J. Geophys. Res.

Abstract.
We examine the balance between processes that contribute to the global and regional distributions of sulfate aerosol in the Earth's atmosphere using a set of simulations from the NCAR CCM3. The analysis suggests that the seasonal cycle of SO_2 and SO_4^{2-} are controlled by a complex interplay between transport, chemistry and deposition processes. The seasonal cycle of these species are not strongly controlled by temporal variations in emissions, but by seasonal variations in volume of air processed by clouds, mass of liquid water serving as a site for aqueous chemistry, amount of oxidant available for the conversion from SO_2 to SO_4^{2-}, vertical transport processes, and deposition. A tagging of the sulfate by emission region (Europe, N. America, Asia, and rest of world [ROW]), chemical pathway (gaseous vs. in-cloud), and type of emissions (anthropogenic vs. biogenic) is used to differentiate the balance of processes controlling the production and loading from this material. Significant differences exist in the destiny of SO_2 molecules emitted from the several regions. An SO_2 molecule emitted from the ROW source region has a much greater potential to form sulfate than one emitted from, for example, Europe. A greater fraction of the SO_2 molecules are oxidized that originate from ROW compared with other areas, and once formed, the sulfate has a longer residence time (that is, it is not readily scavenged). The yield of sulfate from ROW sources of SO_2 is a factor of four higher than that of Europe. A substantially higher fraction of the SO_2 emitted over Europe is oxidized to sulfate through the ozone pathway compared to other regions. The analysis suggests that there are significant differences in the vertical distribution, and horizontal extent, of the propagation of sulfate emitted from the several source regions. Sulfate from Asian source regions reaches the farthest from its point of origin, and makes a significant contribution to burdens in both hemispheres, primarily from plumes reaching out in the upper troposphere. Sulfate from other source regions tend to remain trapped in their hemisphere of origin.

Introduction:

Sulfur emissions from industry, and from natural (biogenic and volcanic) sources are believed to influence the earths climate in a num-

[1]The National Center for Atmospheric Research is sponsored by the National Science Foundation.
Printed: 27 July 1999

ber of ways. Emissions of these sulfur bearing compounds can rapidly form aerosol particles that act to directly modulate the earth's radiation budget by absorbing and scattering radiation (Charlson et al. [1992]), and to indirectly influence many aspects of climate through their interaction with clouds. By serving as cloud condensation nuclei they influence the number and size of cloud droplets, and this has a role in influencing the clouds radiative properties (Twomey [1974]), and the lifetime and precipitation properties of clouds (Albrecht [1989]). Concern about the potential climatic effects of the anthropogenic emission of sulfur species into the atmosphere has motivated numerous studies over the last 10 years [e.g. Chin and Jacob, 1996; Feichter et al., 1996, 1997; Langner and Rodhe, 1991]. In spite of intense study of the atmosphere's sulfur cycle over the last twenty years there are still large gaps and uncertainties in our knowledge about this important component of the earth's climate system.

This paper is the second in a sequence of three describing our efforts to improve our knowledge about the sulfur cycle in the atmosphere. In part I [Barth et al., 1998], we described the basic model used in the studies, compared the model simulation to recent observations of sulfur species, and discussed ways in which the aqueous photochemistry influenced the model sulfur cycle.

In this paper (part II) we adopt a broader view, and describe our model's picture of the life cycle of sulfur in terms of all the processes that control the dominant sulfur species of the atmosphere. Our primary focus is to follow the sulfur atoms as they are emitted (primarily as biogenic DMS or anthropogenic SO_2) through chemical transformation, transport and deposition processes, with the goal of identifying the processes that control sulfate aerosol regionally and seasonally. These controlling processes are revealed by "tagging" of components of the sulfur cycle, in a manner similar to Benkovitz et al. [1994], although their focus was on the North Atlantic region over a two month time span.

In part III, Kiehl et al. [1998] use the model described in the earlier papers to discuss the predicted direct and indirect radiative forcing by aerosols, and the potential for the anthropogenic component to affect climate.

Model description

Several previous studies of the global sulfur budget have been performed in the context of "offline transport models" [Chin et al., 1996; Chuang et al., 1997; Kasibhatla et al., 1997; Langner and Rodhe, 1991; Pham et al., 1995]. The sulfur cycle in the present study evolves within a general circulation model framework. There is significantly more temporal and physical detail available about many processes that influence aerosol formation and their interaction with clouds, climate, and chemistry in a GCM, compared to an offline model. In constrast to offline models where the meteorology is specified by interpolating between snapshots spaced 3 to 6 hours (or even longer) apart GCM solutions are advanced with meteorological information evolving over short (order 20 minute) timesteps. Complete three dimensional distributions of cloud volumes, condensate amounts, and rate of conversion to precipitation, etc. are available in GCMs. Most offline models must approximately reconstruct this information from two dimensional (surface) distributions. The three dimensional fields provide an increased level of consistency with other meteorological information that is difficult to achieve in the offline models. Our GCM configuration is quite similar to that described in Feichter et al. [1996, 1997] or Graf et al. [1997] in the ECHAM4 model. A GCM predicting sulfate that also includes an elaborate representation of the photochemistry of the tropospheric was described in Lelieveld et al. [1997] and Roelofs et al. [1998].

Details of the model are provided in part I, but here we repeat a few relevant points. This

model is comprised of the basic NCAR Community Climate Model (CCM3, [Kiehl et al., 1996]), augmented with a prognostic cloud water scheme [Rasch and Kristjánsson, 1998], and the photochemistry, scavenging, and deposition processes described in part I.

The model is run at the nominal NCAR CCM3 horizontal resolution of 2.8x2.8 degrees, and a variable vertical resolution, with 18 models layers extending from the surface to about 35km. A centered time step of 20 minutes is used for the CCM3 model dynamics, and a consistent approach for cloud and chemistry calculations requires that the transport and most of the chemical processing are advanced from time level $n-1$ to $n+1$ (e.g. a 40 minute time step). This numerical technique can result in a decoupling of solutions at even and odd time steps. Therefore a time filter Asselin [1972] is employed to couple the even and odd time step simulations. The aqueous chemistry is integrated independently using a 2 minute time step to treat the strong sensitivity of the S(IV) + O_3 reaction rates to the time dependent pH evolution. Oxidant distributions, and the H_2O_2 precursor HO_2 in the present model are prescribed from an independent run of the offline transport model IMAGES [Müller and Brasseur, 1995]. The evolution of four chemical species are calculated by the model, DMS, SO_2, SO_4^{2-}, and H_2O_2. The treatment of H_2O_2 is considered important because of the strong interaction of SO_2 and H2O2 in clouds. Most other global models use a "recovery time' (sometimes instantaneous) of H_2O_2 after oxidation and scavenging to a prescribed distribution.

The model represents emissions of DMS and anthropogenic sulfur species (assumed to be 98% SO_2 and 2% SO_4^{2-}) according to the GEIA 1B.1 database following Benkovitz et al. [1996]. Notably lacking are representations for volcanic emissions, and the photochemistry associated CS_2 and COS.

The sulfate aerosol formed by the model would strongly influence the model climate if it were allowed to interact with other physical processes, but in these runs we have deliberately disconnected the mechanisms through which these climate feedbacks could take place. Sulfate is treated as a passive tracer. As mentioned in the introduction, a series of simulations have been made in which the sulfur has been tagged. The runs are of differing length, but all have identical meteorology for a common time period. A seven year run was made in which SO_2 and SO_4^{2-} were tagged according to whether they were of anthropogenic or biogenic origin, and the chemical pathway of formation (i.e. whether the sulfate originated as a result of gas phase or aqueous phase oxidation). A three year run was also made where the constituents were tagged by the region of origin.

The meteorological processes of the CCM3 are thoroughly described in a special issue of the Journal of Climate (Randall [1998] and in Rasch and Kristjánsson [1998],and Bonan [1996]). These collection of papers contain comparisons to clouds, precipitation, winds, boundary layer properties and many other meteorological fields to observational estimates. The CCM is generally quite realistic in its climate simulation, but there are biases that can effect the sulfate simulation. Summertime cloud cover is low over continents (see part III, Kiehl et al. [1998] for some indication of this bias). The amplitude of the seasonal cycle of precipitation over the continental US is often higher than seen in the observations, and precipitiation over Central Europe shows a maximum in spring and a minimum in late fall not seen in the observations which are nearly constant over the year. Generally, the models biases are not larger than those characteristic of other offline CTMs or other GCMs. Differences like these with observations will contribute to bias in all global sulfer models in use today.

Spatial distributions of column burdens of species, and some of the characteristic partitioning by (anthropogenic and biogenic) origin and chemical pathway were shown in part I.

In the following sections we use these tagged properties, along with the region of origin tagging to infer a variety of properties of the atmospheric sulfur cycle as represented in the model.

Global Properties

The distribution of anthropogenic and biogenic emissions of sulfate precursors vary significantly over the globe. Sulfate aerosol from anthropogenic emissions dominates the sulfate column burden throughout the troposphere. For this study, we have partitioned the emissions into four regions defined in table 1. The spatial distribution of anthropogenic emissions is shown in figure 1. Seasonal variations of anthropogenic and biogenic emissions for these regions are displayed in figure 2. The European and American source regions are associated primarily with industrial SO_2 production through coal and petroleum use. The Asian source (which also includes most of the eastern part of Russia) is due primarily to coal burning. The ROW source emissions are often associated with metal smelting operations in the South America and southern Africa region, and with oil processing in middle eastern countries and industry in Australasia. Despite its small geographic area, Europe emits the most SO_2, and has the largest seasonal variation in emission. Emissions from Europe are a factor of 3 higher than those from the ROW region, which has the lowest emission rate despite occupying approximately 6 times more surface area than Europe. Biogenic DMS emissions are small in all regions except the ROW area where they constitute approximately half the total emissions in that region. The ROW DMS emissions peak in southern hemisphere summer.

Figure 3 shows a time series for the 7 year run for SO_2 and SO_4^{2-}. Initial concentrations for these species were set to zero. The atmosphere has been divided up into four layers of approximately equal dry air mass (250 hPa), to show the seasonal cycle of these constituents and their secular trend. The very strong seasonal cycle in SO_2 burdens in the lower troposphere, with a maximum in the lower troposphere during winter is commonly observed in nature, and other models as well. There are regional differences in phase and amplitude of this seasonal variation (discussed in more detail later). The peak in SO_4^{2-} burden is out of phase with that of SO_2 by about half a year.

After transients have died out (*ca.* three years) there are still interannual variations in layer mean burdens of 20%. SO_4^{2-} shows a maximum at all levels in late summer. At this time the SO_2 and SO_4^{2-} are present in substantial amounts at altitudes where scavenging of SO_2 is not effective (because in the present model it is scavenged only in the liquid phase), and where scavenging of SO_4^{2-} acts only through below cloud collection processes. Although the initial transients in the global burden of SO_2 have decayed after the first year, the mass of SO_4^{2-} contained in the upper troposphere and stratosphere continues to increase for the first three years. In these regions timescales of production, mixing and removal are much longer than in the lower troposphere. This result is consistent with other modeling studies in which equilibration in the upper troposphere and stratosphere has been examined. For example, Hartley et al. [1994] required an equilibration time of 1 year in a series of simulations of $CFCl_3$ to calculate the atmospheric lifetime of this constituent, which is photolyzed in the stratosphere. Waugh et al. [1997] found transport times both from modeling and observational data of 0.8 years to the tropical tropopause from the surface, and 3 to 5 years for the signal to reach mid- to high latitudes in the lower troposphere. Our SO_4^{2-} burden in the upper troposphere and stratosphere (order 0.15 Tg S in the uppermost layer) is quite high, significantly higher than that of the comparable study of Graf et al. [1997], but (as shown in Barth et al. [1998]) consistent with the estimated upper troposphere and stratosphere background values of Kent et al. [1994], or the

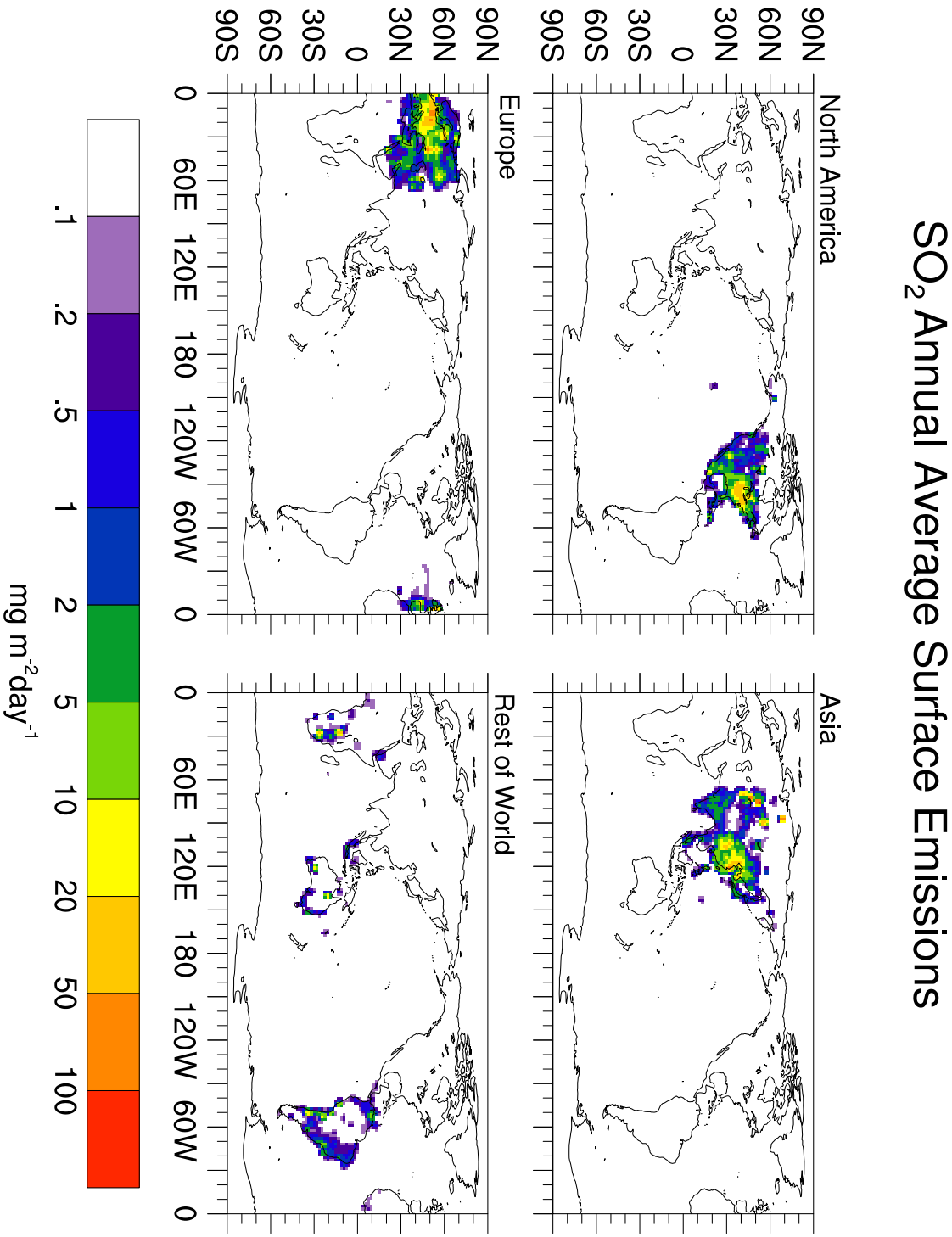

Figure 1. The geographic distribution of annually averaged anthropogenic SO_2 emissions for each of the tagged regions.

Table 1. Definition of regions used in this study

Region	Abbreviation	latitude range	longitude range	% of earth's surface
North America	NA	15-90N	170E-45W	13
Europe	Eu	21-90N	43W-64E	10
Asia	As	0-90N	68-170E	17
Rest of World	ROW	Everthing	else	60

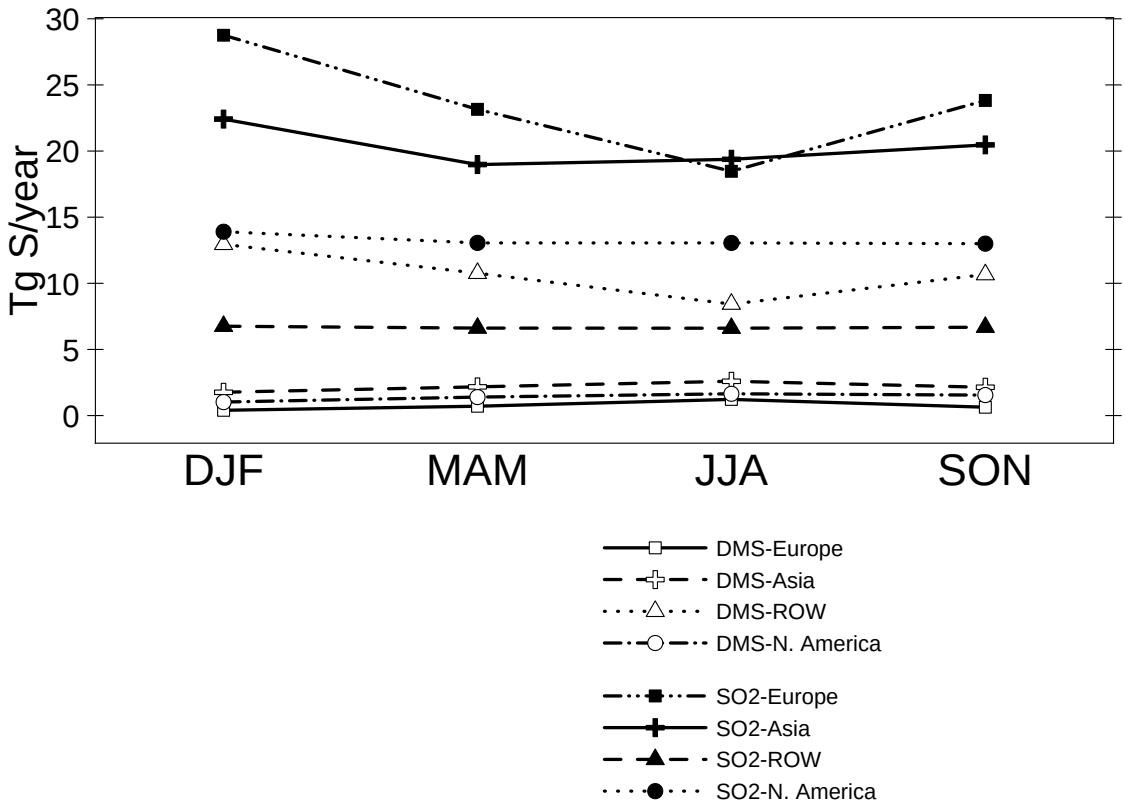

Figure 2. Time series of the seasonal variation in sulfur emissions for the four regions utilized in this study. The lines drawn between seasonal means indicate the linear variation used in the interpolated emissions within the model.

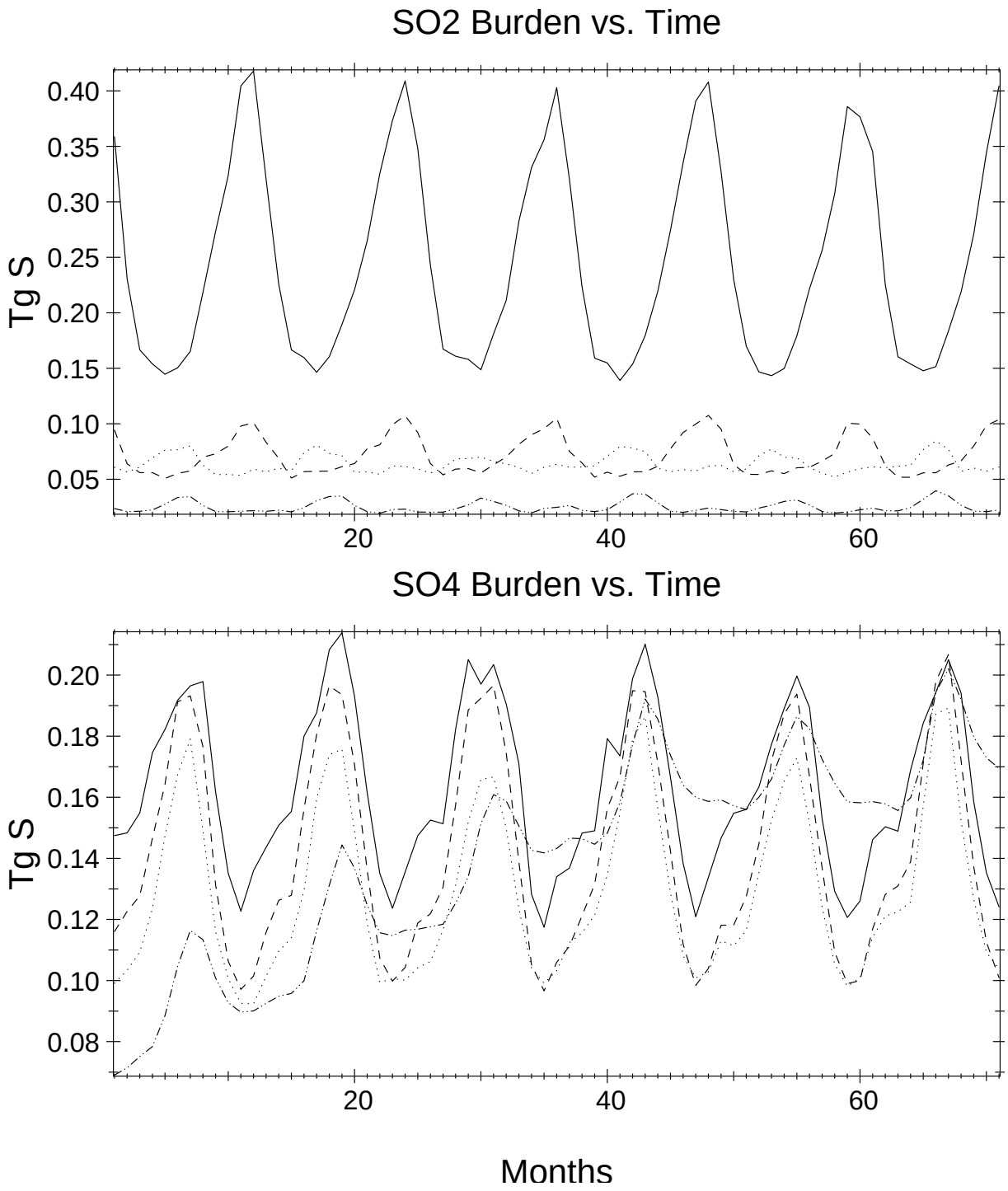

Figure 3. The evolution of the global burden of Sulfur dioxide and Sulfate over the seven year simulation period. The solid line shows the burden in the lowest 250hPa of the atmosphere. The dashed, dotted and dash/dotted lines show successively higher 250hPa layers of the atmosphere respectively. Month 1 corresponds to the first january of the model simulation.

0.12 Tg S for the stratosphere cited in a review paper of stratospheric aerosols by Turco et al. [1982]. The present model is missing much of the relevant photochemistry, and aerosol microphysics for a good representation in this region of the atmosphere, and more precise characterizations of aerosol are required before we can comment more definitively on the upper tropospheric and stratospheric loading. The long time for equilibration in the upper troposphere/stratosphere suggests caution in assessing the upper troposphere and/or stratospheric loadings in runs made over a relatively short period of time [e.g. Benkovitz et al., 1994; Chin et al., 1996; Langner and Rodhe, 1991; Wojcik and Chang, 1997]. If our upper tropospheric burdens of sulfate calculated in this model are indeed too high, other mechanisms for its removal must be investigated (e.g. through scavenging of SO_2 on ice, or aerosol coagulation and settling).

The horizontal distributions of column integrated sulfate for year 3 of our simulations are shown in figure 4. There are very large seasonal variations in column burdens over the primary northern hemisphere emission regions (northeast North America, and Europe) and smaller variations over the widely distributed regions of the southern hemisphere. The burdens from Asian regions are evident year round. The maxima seen during summer/fall periods are consistent with the time series of figure 3. We "tag" the emissions and discuss the controlling processes and propogation from each region later in this study.

Explanations for the seasonal cycle of sulfur species concentrations are complex and vary from model to model. Differences in SO_2 emissions (*cf.* figure 2) are relatively small in the GEIA inventory, except over Europe, where they are higher in winter and lower in summer by about $\pm 30\%$, in response to variations in power and heat usage. (A similar seasonal cycle was prescribed in the emissions used in the other modeling studies cited here.) During winter, in the presence of a relatively stable boundary layer, concentrations of SO_2 become high, and the transformation of SO_2 to SO_4^{2-} may be locally oxidant limited. In summer oxidants are more plentiful, and the venting for the boundary layer can distribute the SO_2 over a larger volume of air, thus exposing it to more oxidant. However, Langner et al. [1992] have noted that observational estimates of cloud amounts used in their model are more abundant during winter and spring in the lower and middle troposphere. Since most of the oxidation takes place within clouds, the decrease in cloud amount in summer will act to oppose the increase in the amount of the aqueous oxidants seen in summer.

The analysis of Feichter et al. [1996] showed that during summer the role of in-cloud and gas phase oxidation played a nearly equal role in converting SO_2 to SO_4^{2-}, but their net effect was significantly smaller than the wintertime oxidation mechanism, where the in-cloud pathway dominated. In principle this would suggest a minimum in SO_2 in the winter and spring, exactly opposite to that seen in observations and most model simulations. Chin and Jacob [1996] indicated that the supply of H_2O_2 was lowest in winter for their model, implying, in the absence of other controlling processes, an effect opposite to the ECHAM simulations. They showed that about 80% of the loss of SO_2 from anthropogenically influenced regions occurred in their model through oxidation and deposition mechanisms and explain their seasonal cycle of SO_2 through seasonal variations in the dry deposition velocity (over snow) and the summer/winter difference in oxidation. Rasch et al. [1998] showed a strong seasonal cycle in SO_2 in two variants of sulfur chemistry in the CCM. One variant used a preliminary, but identical photochemistry to that described in this paper, and the other simply prescribed a uniform oxidation rate of 1.2 days everywhere. Both variants included a seasonally varying deposition velocity sensitive to snow cover, and turbulent and convective venting of the bound-

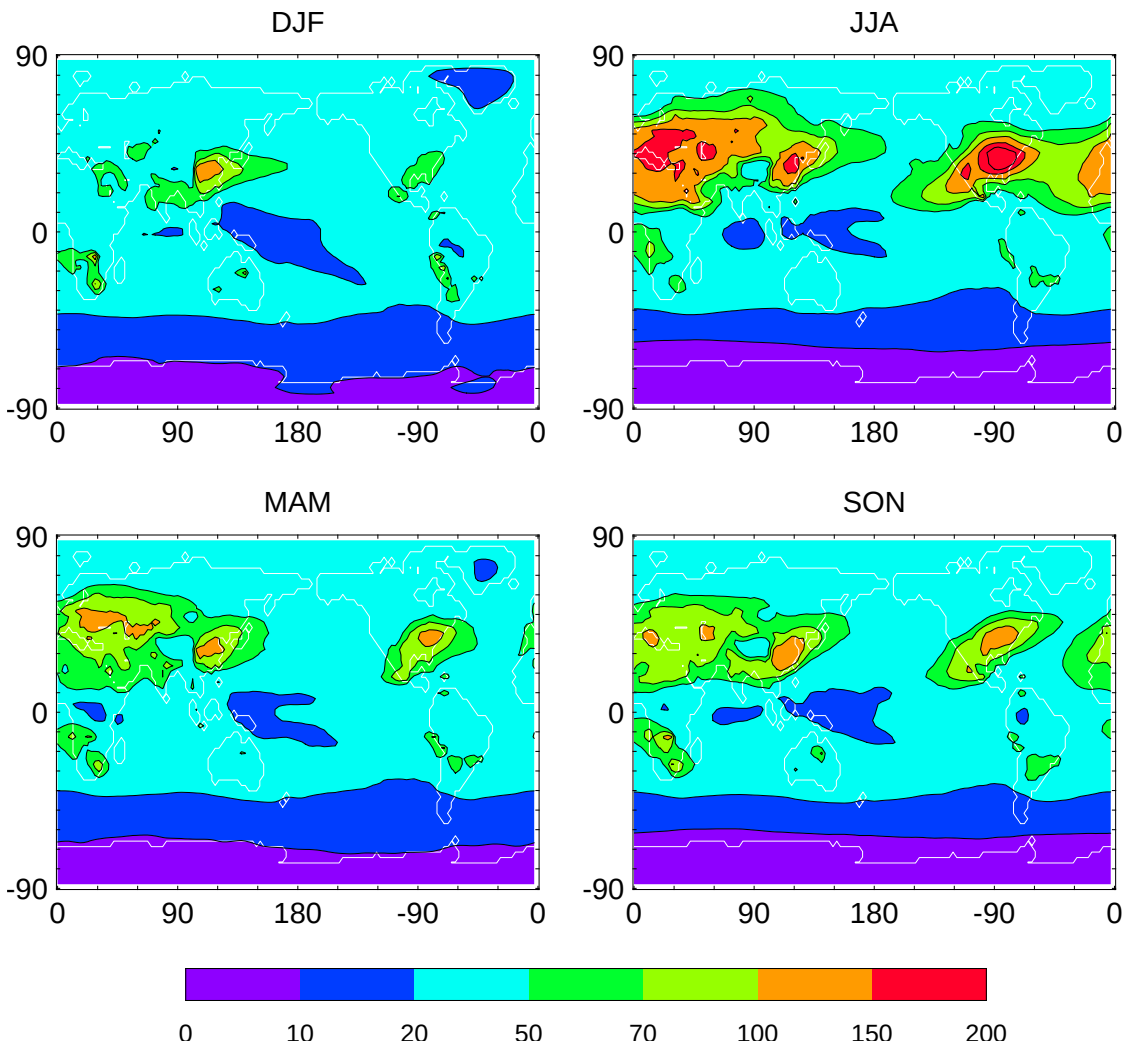

Figure 4. Column burden of sulfate for each season (μmol m^{-2}).

ary layer. Both models showed similar seasonal cycles in SO_2 and SO_4^{2-} burdens, suggesting that the dominant control of the seasonal cycle is not photochemical, but due to susceptibility to scavenging. Kasibhatla et al. [1997] examined the role of variations in chemical conversion in controlling the seasonal cycle of surface SO_2 and SO_4^{2-}. They noted a seasonal cycle of high sulfate in the summer and low sulfate in winter in surface measurements over the US. Surface measurements in Europe did not exhibit this behavior. They suggested the possibility of a (missing) heterogeneous mechanism for the oxidation of SO_2 that takes place year round as a possible needed pathway to explain these differences in the seasonal cycle of SO_2 and SO_4^{2-} over Europe and N. America. Thus, seasonal variations in emissions, available oxidant, cloud volume, transport and meteorological processes, and deposition variations all act to modulate the seasonal cycle of SO_2.

In our model, the winter maxima in the surface layer in SO_2 in figure 3 are also exhibited in the layer extending from 500 to 750 hPa. At altitudes above 500 hPa the seasonal cycle in SO_2 is reversed with a maxima appearing in the NH summer phase, when the SO_2 of surface origin is more easily transported to upper levels. During the summer, the SO_2 is distributed over a larger volume of air that also has higher oxidant availability making its transformation more rapid.

Further indication of the controlling mechanisms for the seasonal cycle in SO_4^{2-} may be found in figure 5, which shows profiles of a variety of quantities averaged over all longitudes between 40N and 90N, as a function of η (the model's hybrid vertical coordinate that corresponds approximately to pressure [in hPa]). This domain was chosen to be large enough that lateral transport in and out of the domain does not dominate the signal, and includes the northern hemisphere source regions where the seasonal variations in burden are largest. The top panel shows summer and wintertime variations in SO_2, SO_4^{2-}, and H_2O_2. SO_2 varies by a factor of 3 between summer and winter in the boundary layer. Peak values are found at about 950 hPa. There is a crossover point at about 400 hPa; above this altitude summer SO_2 values exceed those in the winter. Below this altitude wintertime values always exceed summer. The seasonal differences in SO_4^{2-} amounts disappear by 100 hPa. Above that altitude seasonal variations are also modulated by transport into the stratosphere, which is in turn strongly controlled by stratospheric wave drag, and is a maximum in the NH winter. Since this model has low vertical resolution in the stratosphere, and this strongly affects the quality of the simulation there, and because representations of much of the relevant aerosol precursors, and physics are missing, we do not focus any more on that region. Below 100 hPa the summer:winter ratio for SO_4^{2-} is about 2:1. H_2O_2 exhibits a very strong seasonal cycle, varying by a factor of 3 between summer and winter. As previously mentioned, the strong maximum in H_2O_2 in summer enhances the aqueous oxidation of SO_2 compared to the winter season. Peak H_2O_2 concentrations during summer occur at about 750 hPa. During winter, the peak SO_2 concentrations occur around 400 hPa.

Cloud fraction, total cloud condensate (liquid + ice) and liquid water are shown in figure 5b (the condensate mixing ratios are not in-cloud values, but represent averages over the total [clear plus cloudy fraction of the) grid volume. There are significantly more clouds in the model between 900 and 400 hPa during winter than summer. Since the cloud fraction controls the volume where aqueous oxidation can take place, the higher volumes in winter can enhance oxidation during that season compared to summer. On the other hand, there is significantly more liquid water content in summer. Thus the volume of air susceptible to aqueous processing and scavenging is higher in winter than summer, but the mass of water that participates in the chemistry and scavenging is higher in sum-

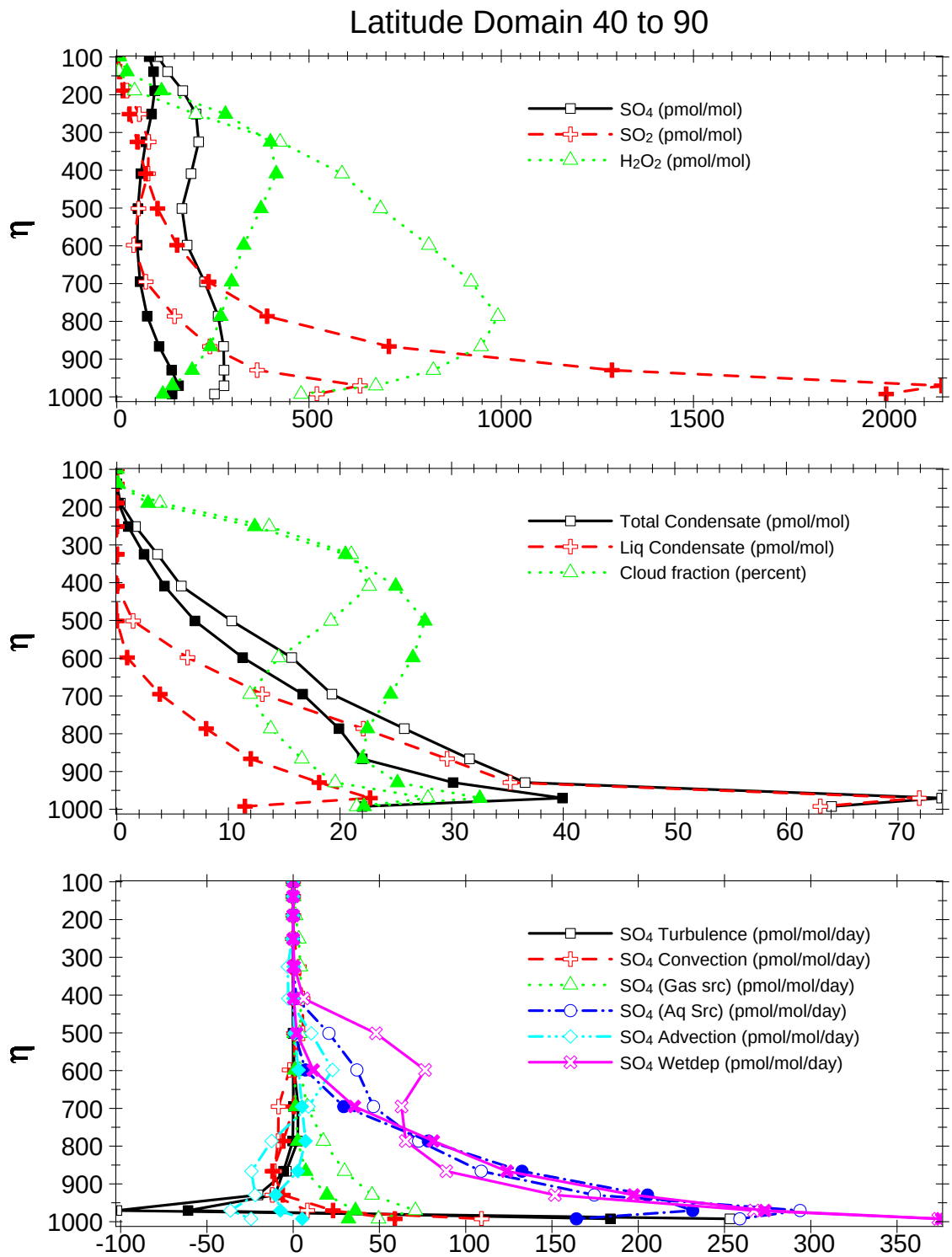

Figure 5. Profiles of many of the terms controlling the seasonal variation of sulfate in the atmosphere, averaged over all longitudes between 40N and 90N. The open (unfilled) markers show the summertime (JJA) values, and closed (filled) markers wintertime (DJF). The vertical coordinate η corresponds approximately to hPa. Note that we have chosen the sign of the wet deposition term to appear as a positive value to emphasize the balance between deposition and production.

mer than winter.

Figure 5c shows the rates of many of the terms involved in the production and removal of sulfate in our model above the surface. Schematically, we represent the sulfate evolution equation as

$$\frac{\partial[\mathrm{SO}_4^{2-}]}{\partial \mathrm{t}} = \begin{array}{l} ADV + TURB + CONV \\ +CHEMA + CHEMG \\ +PR - DRYD - WETD. \end{array}$$

The right hand side of the equation represents the net rate (or tendency) associated with individual processes. ADV represents the advective tendency, TURB represents the net rate of turbulent transport (occuring primarily in the boundary layer), CONV is the rate of convective transport, CHEMA the rate of aqueous oxidation of SO_2 to SO_4^{2-} by O_3 and H_2O_2 , CHEMG the gas phase oxidation rate, PR the rate of primary emission of SO_4^{2-}, and DRYD and WETD the rates of dry and wet deposition processes. At steady state the left hand side of the equation would be identically zero. *Note that we have chosen the sign of the* WETD *and* DRYD *terms to appear as positive values on figures 5 and 7.* The positive sign serves to illustrate the very close balance between WETD and other terms (particularly CHEMA) on the figure. Between 950 hPa and 750 hPa there is a near balance between production from the aqueous pathway and wet deposition during both summer and winter. That is,

$$\mathrm{CHEMA} \approx \mathrm{WETD}. \quad (700\mathrm{hPa} < \mathrm{p} < 900\mathrm{hPa})$$

during both summer and winter. Both processes are more active (by about 20-30%) in our model during winter than during summer in this region, and the aqueous production generally exceeds the wet deposition. The two processes are of course intimately tied to one another as much of the sulfate in formed within the cloud in the same event in which it is removed. The excess production over wet deposition is significantly larger in summer than in winter, contributing to the enhanced sulfate burden in summer. Of course other terms are also important. The gas phase production (CHEMG) adds significantly to the production excess in summer in this region. At altitudes above 700 hPa, and below 900 hPa some aspects of these tendencies are reversed; the aqueous production and wet deposition processes are more active in summer than in winter, and the wet deposition dominates the aqueous production. It is also clear that other processes enter into the total balance in both regions. At altitudes above 700 hPa in summer production by the gas phase term CHEMG, and advection ADV are both important. There is an approximate balance between CHEMA, CHEMG, ADV, and WETD. That is

$$\begin{array}{l} \mathrm{CHEMA}+ \quad CHEMG + ADV \approx WETD \\ \qquad\qquad (400hPa < p < 700hPa) \end{array}$$

in NH summer. Gas phase oxidation shows a substantial seasonal variation from the surface 600 hPa. It is higher by 40-50% in summer than in winter. During winter the balance between 400 hPa and 700 hPa is much like the lower altitude region, except that the wet deposition is the largest term and acts to balance all others.

There are a number of surprising results pertinent to the boundary layer region at pressures greater than 900 hPa. Wet (both below- and in-cloud) deposition in the lowest (100m) layer adjacent to the surface is larger by 30% in winter, and 50% in summer than the next higher layer. The aqueous source term (CHEMA) on the other hand has its maximum in both seasons in the second model layer from the surface (100-300m). This is probably due to the maxima in cloud water and cloud fraction seen in panel 5b, and because SO_2 emissions are above 100m are as large or larger than as those at the surface. Convective transport (CONV) and turbulent transports (TURB) of aerosol are both important in the boundary layers with large positive amplitude in the near surface layer, and negative values higher up. Thus, these terms act

to transport aerosol from higher levels *downward* and into the surface layer where it is susceptable to strong removal by dry deposition processes (not shown) and wet scavenging. Convective transports are usually thought to act to move constituents out of the boundary layer. In the case of soluble species however (at least as represented here), the upward transport inside the updraft cores of any aerosol remaining after scavenging, is overwhelmed by the compensating downward transports of unscavenged aerosol in the environment. Advection (ADV) by resolved scale processes (*i.e.* not turbulence) generally acts to move the sulfate from the near surface layers both upward, and laterally (in this case southward). During the summer, advection acts as a significant source to the region from 700 hPa to 500 hPa. During winter it acts mostly to move SO_4^{2-} out of the domain. Within cloudy volumes non-advective processes dominate the advection term, but in cloud free regions advection is important, and its enhanced role in summer time must be due to the larger volume of cloud-free air during that season.

The column integral of each term for the same domain are shown in figure 6 on a month by month basis. The seasonal variation of these quantities show interesting differences with the corresponding quantities shown in figure 1 of Feichter et al. [1996]. Their simulations indicated a maximum in oxidation via H_2O_2 in March and April, and a minimum (of 0.7 Tg S/mo) in June and July. The present model exhibits a similar maximum, but the minimum in JJA is much smaller than the simulation of Feichter et. al. The shape of the seasonal cycle in the gas phase production of Feichter et. al. is quite similar to the present model but their maximum in summer is approximately twice as large as that found here. Feichter et al found a maximum in surface deposition in the fall, where the maxima is in the spring in the present model. The differences in the two models portrayal of seasonal variations in processes again highlight our current uncertainty in understandings of the atmospheric sulfur cycle.

When the region of integration is restricted to the region of strongest emissions, the balances change, compared to the larger northern hemisphere region. Figure 7 shows the corresponding profiles over Eastern North America. As should be anticipated, the vertical gradient of SO_2 and SO_4^{2-} is larger over the source region, and near surface values are a factor of two higher. Summertime values of SO_2 are higher than wintertime values at all altitudes above 800 hPa. The mass of liquid condensate is substantially lower over this area than the northern hemisphere in general. Unlike the larger region there is more total condensate in winter than summer, although there is still much more liquid condensate in summer than winter. The difference between summer and winter cloud fraction is also much larger. All tendencies tend to be a factor of two higher in the smaller source region, than averaged over the larger domain. Lateral advection of sulfate out of the domain is also more apparent. There is a net vertical transport into the region from 500 to 700 hPa by resolved scale advection from below. As also seen over the larger region, the gas phase oxidation shows a substantial seasonal variation from the surface 600 hPa. It is higher by 40-50% in summer than in winter. This result differs from a similar analys in the model study of Chin and Jacob [1996] who found no variation in the rate of summer and winter production of sulfate by gas phase photochemistry in the lower troposphere. The difference between summer and wintertime production by aqueous oxidation is also substantially larger over this region than the larger domain discussed above. Both sulfate and SO_2 are transported to the mid- and upper troposphere by convection, despite of their solubility, and the convection term is significantly larger over this (primarly) continental region than it is over the larger domain. Convection and oxidation of SO_2 by OH are sources for sulfate between 200

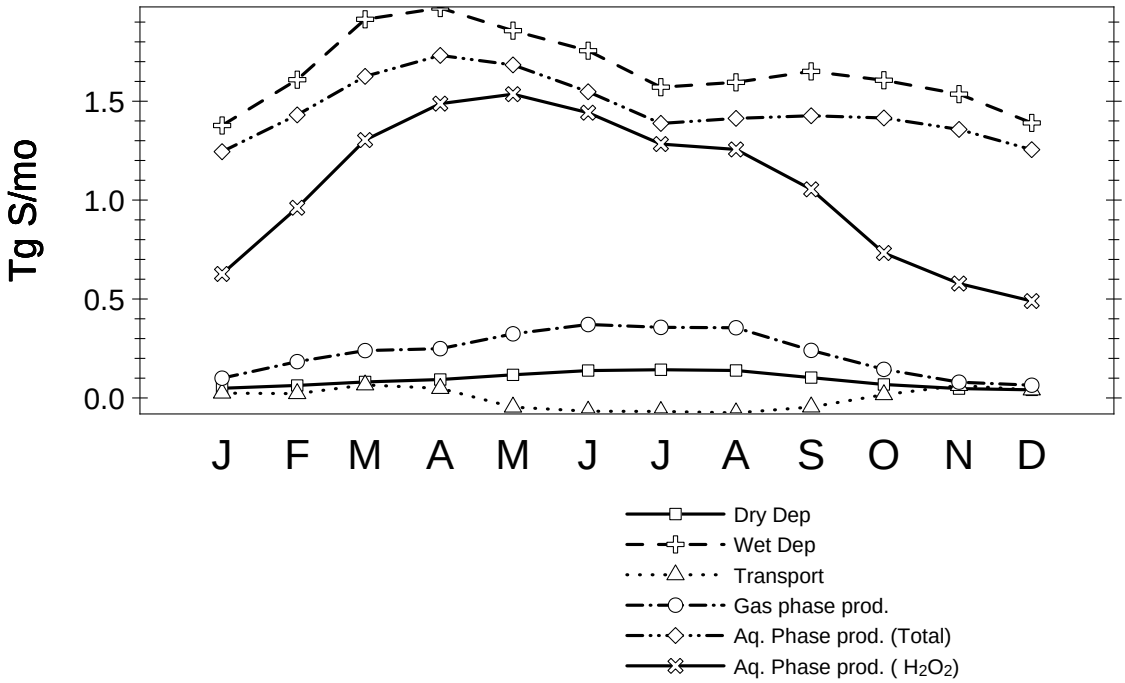

Figure 6. Time series of many of the terms controlling the seasonal variation of sulfate in the atmosphere, averaged over all longitudes between 40N and 90N.

and 500 hPa in summer. These source terms for sulfate at heights above 500 hPa are balanced by advection which acts to transport the sulfate elsewhere. Between the surface and 700 hPa, sources of SO_4^{2-} by aqueous and gaseous oxidation substantially (by about 100%) exceed the wet deposition process, the remaining excess of production is export from this region by advective processes, particularly during summer.

Global budgets for the present model and several other recent model studies are shown in tables 2 through 4. These studies are certainly not a comprehensive list, but they provide a general picture of the current range of variation in global modeling. Three of the models (Langner and Rodhe [1991], Pham et al. [1995] and Chin et al. [1996]) are offline models characterized by relatively simple formulations for transport, convection and cloud processing, necessitated by the lack of much of the information required for a more elaborate formulation (none of these models had access to 3 dimensional distributions of cloud variables for example). The studies of Feichter et al. [1996] and Roelofs et al. [1998] are quite similar to ours. They also utilized a general circulation model in which the model hydrological cycle, cloud volumes for chemical processing, etc. were handled on short time scales in an internally consistent way. Some of the prior studies included additional source terms (volcanoes and biomass burning) neglected in our study. On the other hand, some of the cited studies have treated a smaller number of oxidation pathways (for example by neglecting reactions with O_3). Only the model described in Lelieveld et al. [1997]; Roelofs et al. [1998] have as elaborate a treatement of the production and loss of H_2O_2.

The lifetime of DMS (table 1) varies considerably among the several models. Langner and Rodhe [1991] did not include the NO3 oxidation pathway, and assumed all DMS + OH went to SO_2. Their lifetime is the longest of the cited models. Chin et al. [1996] postulated, and

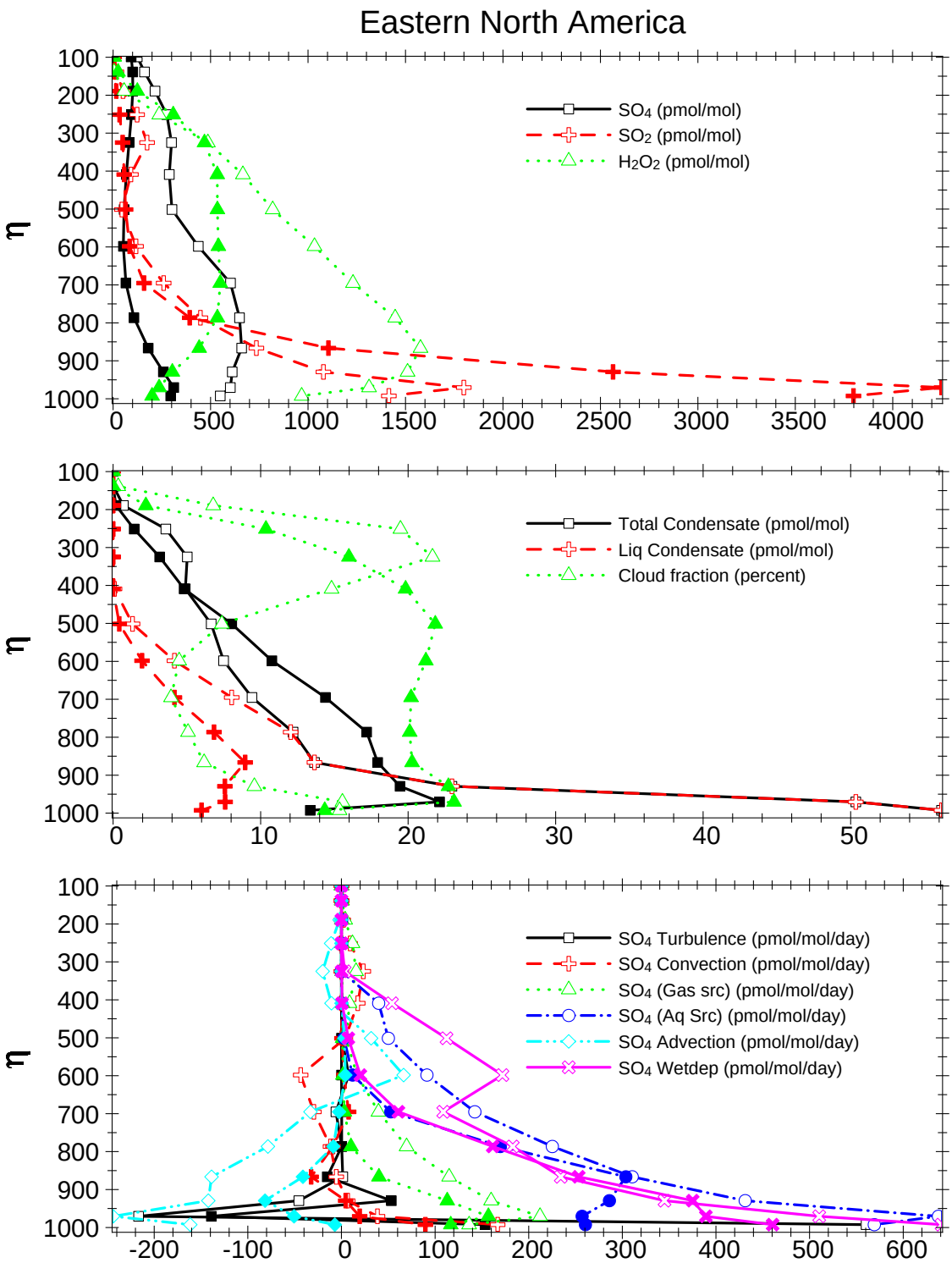

Figure 7. Profiles of many of the terms controlling the seasonal variation of sulfate in the atmosphere, averaged over Eastern N. America (60W-90W, 30-60N). The open (unfilled) markers show the summertime (JJA) values, and closed (filled) markers wintertime (DJF). The vertical coordinate η corresponds approximately to hPa.

Table 2. Global annual averaged DMS budgets for years 3-6 compared to other model studies. Previous studies are abbreviated as follows: LR91 = Langner and Rodhe [1991], P95 = Pham et al. [1995], F96 = Feichter et al. [1996], C96 = Chin et al. [1996] L97 = Lelieveld et al. [1997].

Quantity (Units)	LR91	P95	F96	C96	L97	This work
Source (Tg S/yr)	16	20	17	22	16	16
Burden (Tg S)	0.13	0.05	0.10	0.06	0.02	0.06
Lifetime (Days)	3	0.9	2.2	1.0	0.5	1.42

used, a missing oxidation path for DMS in order to achieve a reasonable agreement with observations. The additional pathway reduced the DMS lifetime substantially. It is interesting to note that the studies of Feichter et al. [1996] and Lelieveld et al. [1997], which use the same fundamental meterological description and aerosol chemistry, differ by a factor of four in the DMS lifetime (2.2 vs 0.5 days respectively). The difference is presumably due to variation in OH distributions. The present model lies between those model results.

With respect to SO_2 , the present study, which lacks volcanic emissions, biomass burning, and CS_2 and COS sources has the lowest source strength for SO_2, and thus anthropogenic emissions appear as a relatively higher fraction of the source in table 3. The three models using a prognostic cloud water variable, and interactive clouds tend to lose more SO_2 by gas-phase oxidation than the models containing simpler formulations for clouds. These studies also limited the SO_2 oxidized by H2O2 more strictly than the studies of Chin et al. [1996] and Pham et al. [1995]. There is an order of magnitude of variation in wet deposition of SO_2 between models, ranging from the present study and Lelieveld et al. [1997]; Roelofs et al. [1998] at the low end (2% and 0% respectively) to that of Chin et al. [1996] at the high end (21%). This is likely to be a explained as a labelling issue. The partitioning of the SO_4^{2-} that has not yet existed as a aerosol [S(VI)] can be distinguished from that arising from ingestion of a pre-existing soluble aerosol by a precipitating cloud drop. Our wet deposition of SO_2 refers only to the deposition of S(IV). The balance is attributed to deposition as sulfate. As such, our numbers are quite consistent with the numerous observational estimates cited in Wojcik and Chang [1997]. Part I [Barth et. al, this issue] (figure 6) suggests that our model agrees quite well with observations of total wet deposition (SO_2 + SO_4^{2-}) and thus the descrepancy among models is likely just a labelling issue. Langner and Rodhe [1991] also included the enhanced uptake of SO_2 in solution due to complexation with formaldehyde. The sum of the wet deposition and aqueous oxidation provides an estimate of loss of SO_2 through cloud processing. There is still a large variation between these fields among models, and the two models with the most internal consistency in treatment of physical processes are very different in this sense (43% vs. 58% respectively). The two models with predicted H_2O_2 distributions have the longest lifetime for SO_2. The depletion of H_2O_2 in near-source regions can result in a decrease in the rate of production of SO_4^{2-}. Part I showed that there was often an appreciable length of time for replenishment of the H_2O_2 after it was depleted through oxidation and precipitation scavenging. This would increase the frequency of situations where SO_2 is limited to the slower O_3 reaction for its oxidation pathway. (Not allowing the H_2O_2 depletion results in an increase of order 7% in the production of SO_4^{2-}.)

Table 3. Global annual averaged SO_2 budgets for years 3-6 compared to other model studies. Previous studies are abbreviated as follows: LR91 = Langner and Rodhe [1991], P95 = Pham et al. [1995], F96 = Feichter et al. [1996], C96 = Chin et al. [1996] L97 = Lelieveld et al. [1997].

Quantity (Units)	LR91	P95	F96	C96	L97	This work
Source (Tg S/yr)	95	123	101	96	90	79
Anthro. emissions (%)	71	75	78	68	74	82
Photochemical prod. (%)	18	15	17	23	18	18
Other (%)	11	10	6	9	8	0
Gas phase oxidation (%)	8	5	17	8	15	12
In-cloud oxidation (%)	44	45	34	44	59	56
Wet deposition (%)	15	4	9	21	0	2
Dry deposition (%)	32	45	40	28	24	31
Burden (Tg S)	0.3	0.2	0.4	0.3	0.6	0.4
Lifetime (Days)	1.2	0.6	1.5	1.3	2.3	1.9

Table 4. Global annual averaged SO_4^{2-} budgets for years 3-6 compared to other model studies. Previous studies are abbreviated as follows: LR91 = Langner and Rodhe [1991], P95 = Pham et al. [1995], F96 = Feichter et al. [1996], C96 = Chin et al. [1996] L97 = Lelieveld et al. [1997].

Quantity (Units)	LR91	P95	F96	C96	L97	This work
Source (Tg S/yr)	53	62	51	49	72	55
Anthro. emissions (%)	6	0	0	0	5	2
Gas phase production (%)	15	10	33	15	21	17
In-cloud production (%)	79	90	67	85	74	81
Dry deposition (%)	16	27	13	11	25	7
Wet deposition (%)	84	73	87	89	75	93
Burden (Tg S)	0.8	0.8	0.6	0.53	1.1	0.60
Lifetime (Days)	5.3	4.7	4.3	3.9	5.3	4.0

Despite the large differences in emission inventories, photochemistry, cloud properties, and deposition parameterizations for SO_2, the net source for SO_4^{2-} from all the models varies by only 20% (table 4), with the exception of the model described in Lelieveld et al. [1997]; Roelofs et al. [1998], which has a signifiantly higher source value. The partitioning between aqueous and gas phase production varies substantially between models. All models show the aqueous pathway to dominate, but there is no consistent signature between models with the more elaborate treatments for clouds and oxidation, and the simpler formulations. This suggests again that there are still very large uncertainties in the characterization of the atmospheric sulfur cycle.

Regional Analysis

It is now generally accepted that emissions from the industrial nations of the northern hemisphere are the dominant source of tropospheric sulfate in the world today. Yet the relative contribution of the several source regions to the global sulfur budget, and possible differences in the processes that control the sulfur distribution from these regions remain poorly understood. In this section we make use of tagged aerosol types to make infererences about the effect of emissions from the different regions.

The partitioning of the annually averaged regional emissions and burdens into their anthropogenic and biogenic components can be assessed from the bar charts of figure (8) and (9). Anthropogenic emissions dominate over biogenic emissions in all regions except ROW, where they are of similar magnitude. In the northern hemisphere, more than 80% of the total burden is due to anthropogenic sulfate. However, even in the southern hemisphere, the anthropogenic sulfate is generally more than 50% of the total burden. In the tropical region of the Pacific Ocean, sulfate aerosols derived from DMS emissions and anthropogenic sulfate contribute equally to the total burden. These results contrast with Chin and Jacob [1996], who found a larger contribution from non-anthropogenic sources, particularly in the southern hemisphere and oceanic regions. These differences could arise because in our model DMS emissions are less than those used by Chin and Jacob [1996] and because our model does not include volcanic emissions of SO_2 , or because Chin and Jacob [1996] determined the anthropogenic contribution by comparing simulations using only natural emissions to a simulation with present day natural and anthropogenic emissions. We have also made similar pre-industrial and present day runs, and we believe that most the differences between our simulations and those of Chin and Jacob [1996] cannot be explained by the non-linear reponse of the chemistry and scavenging to the changing emissions.

Although the ratio of anthropogenic to biogenic emissions in the northern hemisphere regions of Eu, NA, and As are approximately 10:1 or greater, the burdens of resulting sulfate are order 5:1 for the corresponding regions. That is, the yield of sulfate is higher from biogenic precurson emissions than from anthropogenic precursors. Hence, sulfur emitted from biogenic sources is converted to sulfate (relatively) more efficiently than that emitted from anthropogenic sources. This is easily explained (Chin and Jacob [1996] and Feichter et al. [1997]) by the rapid transport from the surface to the upper troposphere of the quite insoluble DMS, where it is subsequently oxidized to SO_2 and SO_4^{2-}. Sulfate produced in the upper troposphere is not easily susceptable to scavenging, and must first be transported downward to altitudes where removal processes are more efficient. It is also evident from figure 9 that there are significant differences between the relative partitioning between SO_2 and SO_4^{2-} among the regions. While there is more sulfur stored as SO_4^{2-} in the NA, Asian, and ROW regions, the situation is reversed in Europe. These features suggest significant differences in transport, transformation,

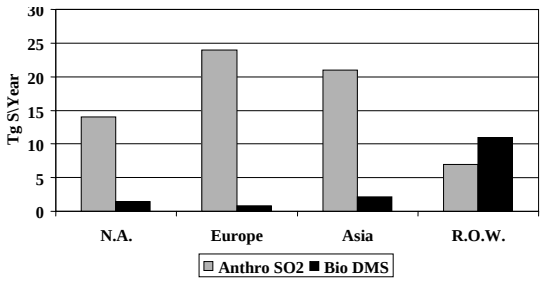

Figure 8. Annual emission of sulfur speciecs by region, partitioned by anthropogenic and biogenic emissions.

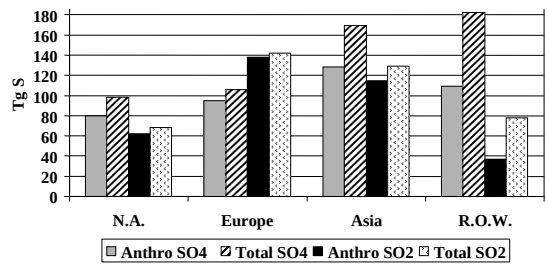

Figure 9. Annually averaged burden of sulfur species by region, partitioned into anthropogenic and total contributions.

and deposition mechanisms over the four regions (discussed below).

The point can be made more strongly by considering what we term the *Potential* or *Susceptability* of a region to emissions. This is defined to be

$$\text{Potential} = \frac{\text{SO}_4 \text{ aerosol burden}}{\text{near surface sulfur emission}}.$$

Thus, the sulfate potential defines the yield of aerosol per unit emisssion of sulfur as SO_2 or DMS.

Figure 10 shows that anthropogenic emissions from the ROW have more potential for aerosol formation than other regions. A kilogram of sulfur emitted as SO_2 from a ROW source will produce approximately four times more aerosol than the same kilogram of SO_2 emitted over Europe, which has the lowest potential for sulfate formation according to our model. The Asian region is intermediate to

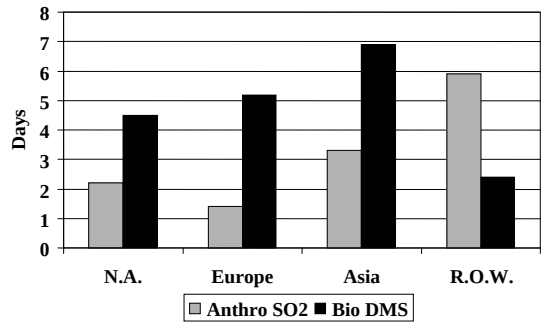

Figure 10. Sulfate potential, defined as the Sulfate burden (Kg S) resulting from a unit emission of sulfur (Kg S/day) at the surface.

the others in this susceptibility to aerosol formation. The sulfate potential does not identify what process or processes control the distribution and amplitude of the aerosol mass, it just defines the potential for a given emission of a sulfur atom from a region to end up as sulfate mass.

The controlling processes can be identified by a consideration of ratios of other quantities available from the model. Figure 11 shows the sulfate lifetime (defined as the ratio of the sulfate burden to the total deposition flux). This quanitity is the inverse of the rate at which sulfate (arising from emissions from a given region) is removed from the atmosphere. The diagnostic suggests that part of the explanation for the potential is associated with deposition processes. Sulfate arising from anthropogenic ROW sources has a lifetime against deposition of about 6 days, and is not deposited as readily as sulfate from other regions at the surface. Also, unlike the other regions, the lifetime of biogenic sulfate from that region is actually shorter than that of the anthropogenic component. The vertical distribution of the anthropogenic ROW sulfate is nearly uniform, somewhat like DMS and thus ROW aerosols are not so susceptible to scavenging. We believe that this is because the ROW sources are in close proximity to regions of vigorous continental year round convection (e.g. Amazo-

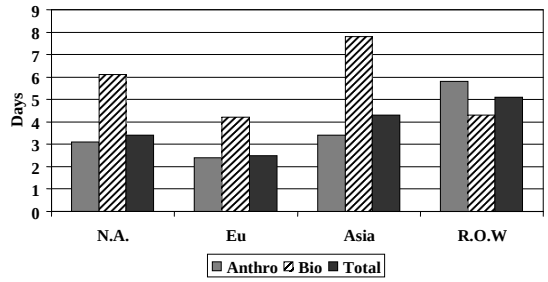

Figure 11. The lifetime of Sulfate emitted from each region.

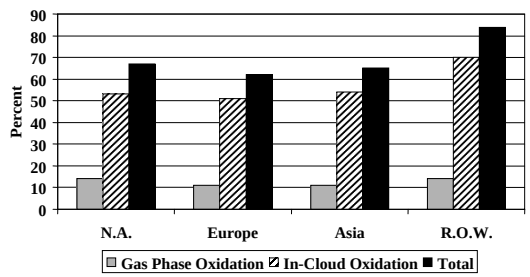

Figure 12. The fraction of SO_2 emitted from each region that is converted to SO_4^{2-}.

nia and South Africa) that transports the SO_2 rapidly to the upper troposphere.

Figure 12 shows the sulfate yield as a fraction of emitted SO_2 that produces sulfate. The balance of the SO_2 undergoes wet or dry deposition. The ROW SO_2 emissions result in 15-20% greater yield than do emissions from other regions. This total yield can in turn be partitioned into aqueous and gas phase oxidation components. Thus ROW sources are converted more efficiently to sulfate, and are subject to less efficient surface deposition than other regions. Also, the ratio of aqueous to gaseous oxidation is also slightly higher in ROW than other regions.

Figure 13 partitions the aqueous oxidation pathways according to the fraction oxidized by H_2O_2 or O_3. Europe stands out from the other regions by having a much higher (factor of 2)

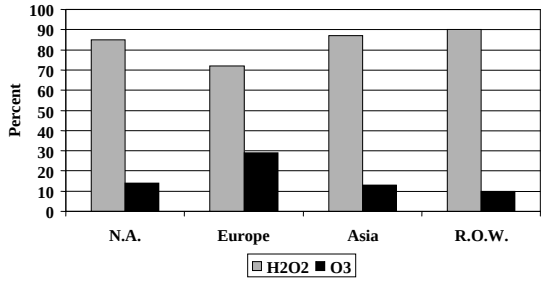

Figure 13. The fraction of oxidation taking place by the two primary aqueous phase pathways.

fraction of the sulfate produced by the O_3 pathway. This suggests that the European region exists in a peroxide limited situation much more frequently than any of the other model regions. This can be attibuted to the much higher emissions densities over Europe compared to any of the other defined areas. Also, because Europe is located at higher latitudes than the other regions, there is less oxididant availability, and reaction rates are slower. This effect is most pronounced in winter when the European emissions peak.

Spatial and seasonal distributions from regional emission

The horizontal spatial distribution of each of the annually averaged regionally tagged sulfate types are shown in figure (14). The left column shows the column burden from each emission region, and right the percent of the total column burden contributed from each region. In the interest of brevity we do not show, but will discuss, the seasonal variation of the regionally tagged sulfate. There is a strong seasonal variation for Europe and North America, with summer to winter ratios for peak values of about 4:1 over both regions. The plume emitted from North America extends eastward following the storm track, and carries approximatly a factor of two more sulfate over the Atlantic in

summer than in winter. The peak amplitudes over the North American and European emission regions are quite similar to those described by Feichter et al. [1996] and Kasibhatla et al. [1997]. Another plume from the southwest US and Mexico areas is also evident during summer. The plume (also seen in Benkovitz et al. [1994]) extends westward in the subtropics and carries significant amounts of sulfate across the pacific as far as Hawaii. This plume is significantly stronger than that seen in Feichter et al. [1996]. The model evaluation of part I suggests it is probably too strong. The Asian emissions generate burdens that are quite similar to Feichter et al. [1996] but significantly greater than those seen in Kasibhatla et al. [1997]. There is little seasonal cycle in maximum amplitude but the extent of the area occupied by a high sulfate burden is significantly larger in NH summer than in winter. There are much smaller variations between summer and winter burdens from the ROW emissions. Burdens of 60 $\mu mole/m^2$ during summer are a factor of two larger than during winter.

The picture changes somewhat when viewed as a percentage. Asian emissions (including those from Siberia) contribute most strongly to burdens in the NH polar regions during winter; during summer European sources contribute most strongly. North America appears as a distant third place contributor in all seasons. Very little ($<$ 10%) of the sulfate derived from emissions from North America or Europe penetrate into the southern hemisphere. Similarly, very little of the sulfate from ROW emissions contribute the northern hemisphere. Asia, on the other hand contributes in an important way to the burden in both the northern and southern hemispheres. It reaches the southern hemisphere most efficiently in the JJA season where it comprises 20-40% of the burden in the subtropics. Although this contribution to the southern hemisphere is quite small in magnitude, it indicates a pathway for transport from anthropogenic sources of potential importance in the future. The ROW sources reach to about 30N during NH winter where they comprise approximately 30% of the column burden there.

Seasonal cycles of the SO_4^{2-} burdens in each vertical quartile (250 hPa layer) are shown in figure 15 for each emission region. The largest burdens result from European emissions with summer to winter ratios of about 2:1. Burdens from European emissions fall off with increasing altitude more strongly than any of the other regions. Asian and ROW burdens have the least seasonality and stratification.

Latitude-height cross-sections of zonally averaged sulfate from each region are shown in Figure 16. The largest lower tropospheric values are associated with the European emission region during NH summer. The sulfate aerosol remains at low altitudes for the European source region, in contrast to a penetration of relatively large sulfate loadings to higher altitudes from North American and Asian sources. The Asian source emission contribute the most to the north polar region during Northern summer. The ROW source is much more uniformly distributed in the vertical, and shows little seasonal variation. The emission regions associated with areas of vigorous deep convection tend to have significantly higher burdens aloft. The sulfate from all source regions show a spreading of contours with altitude, indicating that once aloft, the aerosol is less susceptable to removal processes and so can travel great distances unimpeded. This tendency is evident for each panel in the figure. Asian emissions are most important to the supply of upper tropospheric sulfate in the northern hemisphere, and the only important northern hemisphere source region reaching to the southern hemisphere. The Asian source region is responsible for more than 40% of the sulfate above 400 hPa in the northern hemisphere. North American and European sources are trapped in the northern hemisphere and contribute less than 10% to the aerosol amount at any altitude in the opposite hemisphere.

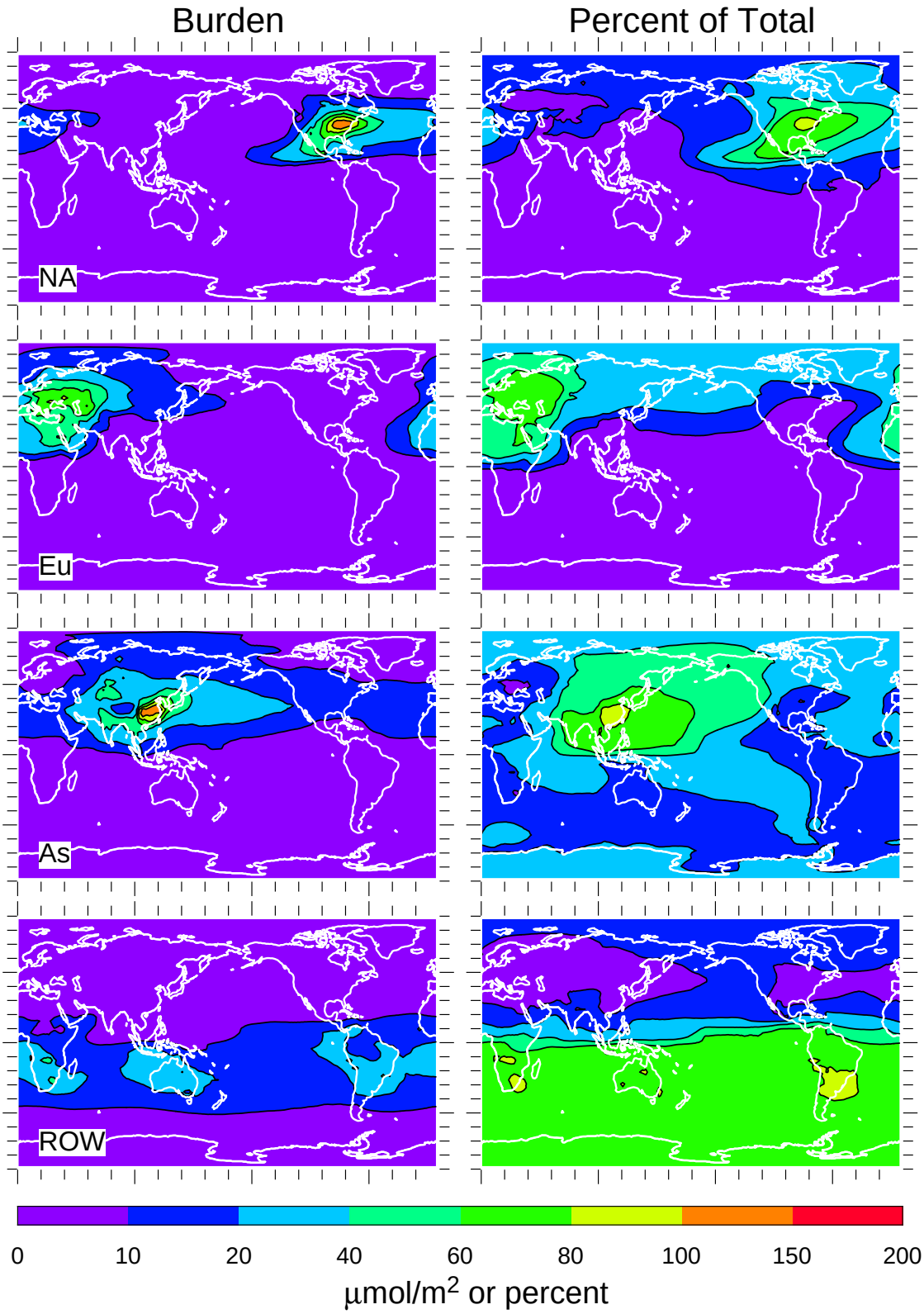

Figure 14. Annually averaged column burden of sulfate for the four regional emissions (indicated in the lower left corner of each panel), expressed in μmol/m^2 in the left column, and as a percent of the total burden in the right column.

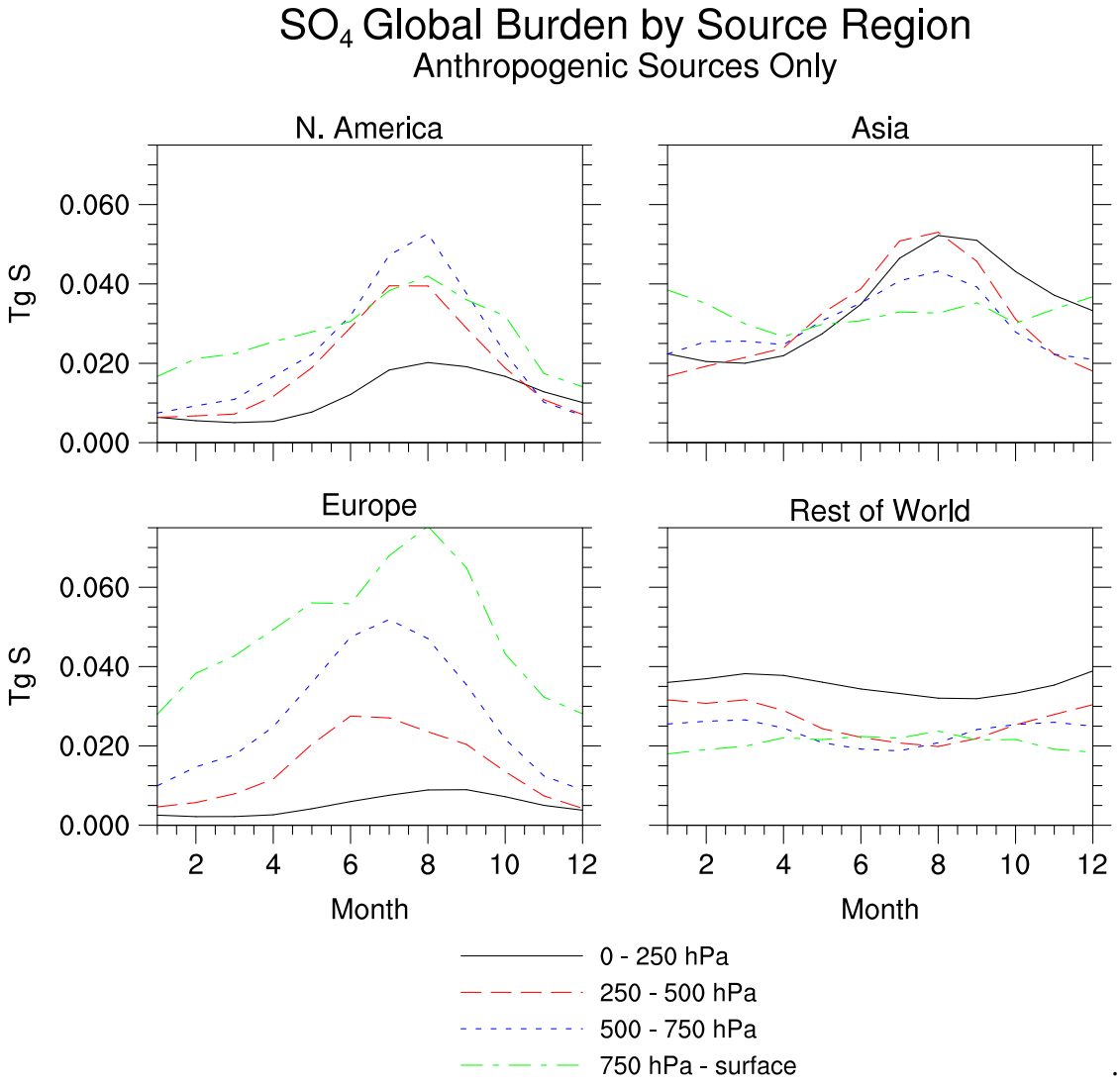

Figure 15. Time series for year 3 of the sulfate burden stratified by layer for each region.

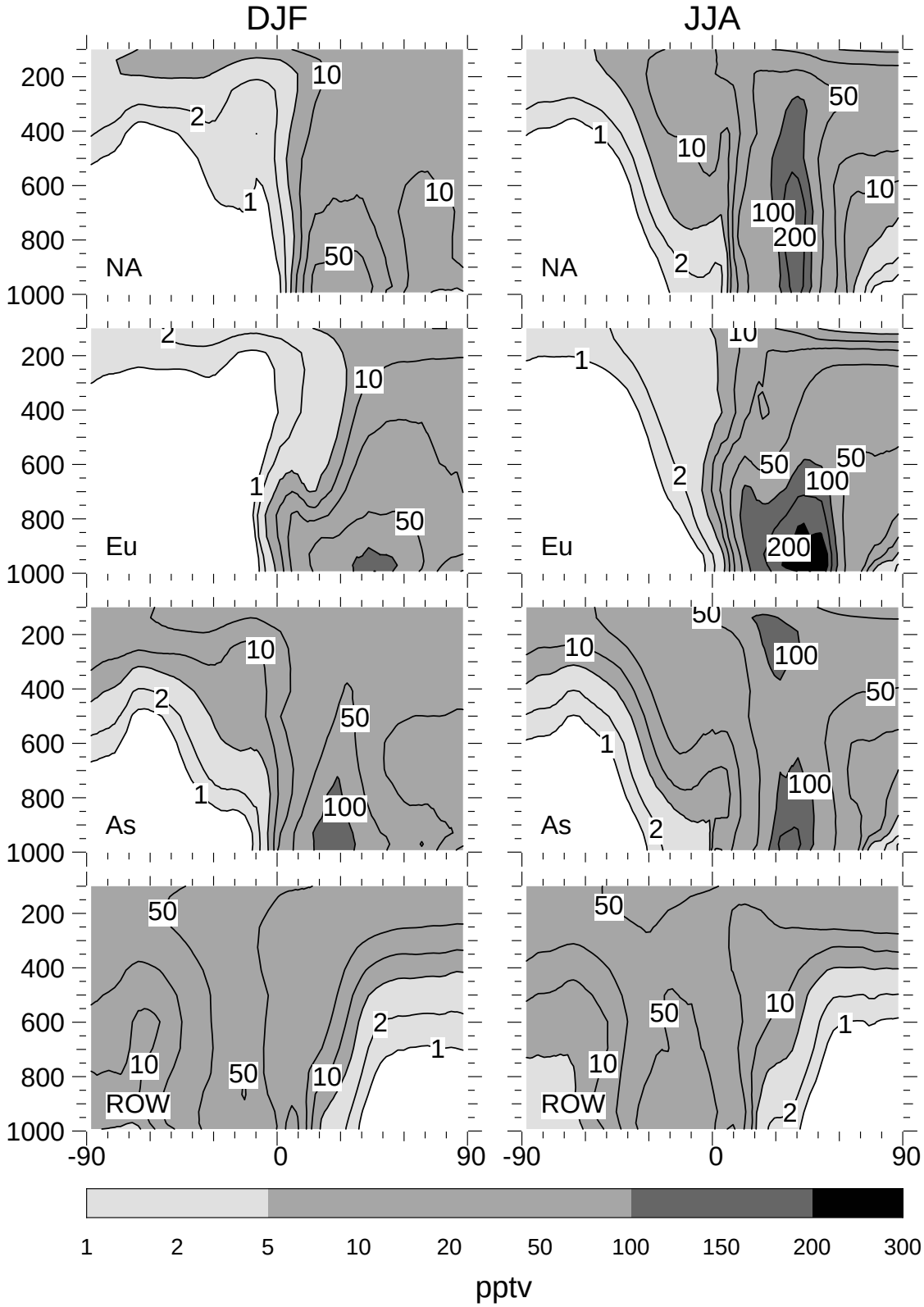

Figure 16. Zonal average of sulfate distribution for the four regional emissions (biogenic + anthropogenic, regions indicated in the lower left corner of each panel) for DJF (left column) and JJA (right column). Shading and contours are indicated at the bottom of the figure.

Summary and Conclusions

We have examined the balance between processes that contribute to the global and regional distributions of sulfate aerosol in the Earth's atmosphere, using a set of simulations from the NCAR CCM3. The model, the sensitivity to its chemical formulation, and comparisons to observations are described in detail in part I (Barth et al. [1998]). The radiative forcings that arise from these simulations are analyzed in Part III (Kiehl et al. [1998]).

The analysis suggests that the seasonal cycle of SO_2 and SO_4^{2-} are controlled by a complex interplay between transport, chemistry and deposition processes. The seasonal cycle of these species are only weakly influenced by seasonal variations in emissions. Rather, they are controlled by seasonal variations in volume of air processed by clouds, by mass of liquid water serving as a site for aqueous chemistry, by amount of oxidant available for the conversion from SO_2 to SO_4^{2-}, and by variations in vertical precipitation and transport processes. Three separate processes contribute to vertical transport: 1) advective processes resolved by the present model, 2) transport by subgrid-scale convection, and 3) transport by subgrid-scale turbulent processes in the boundary layer. The primary removal mechanism for sulfate is wet deposition. Both gaseous and aqueous production of aerosol is substantially higher in the summer in the lower troposphere (surface to 3 km) than in winter. The enhancement is probably due to more clouds in the liquid phase and higher oxidant concentrations. Wet deposition has a strong seasonal variation in the near surface layer (surface to about 1km), but very little variation between 1 and 3 km. The excess production between 1 and 3km leads to an enhanced burden at these altitudes. At higher altitudes, the balance of processes becomes more complex, with vertical transport processes also playing a role. There is significant convective transport of SO_2 and SO_4^{2-} during summer. Resolved-scale advection in cloud-free areas also plays a role during summer, but not winter. This suggests that the resolved vertical advection during summer is taking place in the cloud-free regions (which are larger in summer); in cloudy regions the wet deposition tends to reduce the importance of the resolved vertical transport. The seasonal behavior and balance of processes in our model differ in many ways from those found in model studies by Feichter et al. [1996] and Chin and Jacob [1996]; we do not believe there are sufficient measurements to identify which of these studies is most realistic. The differences highlight the uncertainty in the processes responsible for sulfate's seasonal behavior. More work is need to resolve these discrepancies.

A tagging of the aerosol by emission region (Europe, N. America, Asia, and the Rest of World), chemical pathway (gaseous vs. aqueous), and type of emissions (anthropogenic vs. biogenic) was used to differentiate the balance of processes controlling the aerosol resulting from the emissions. The analysis suggests that significant differences exist in the destiny of SO_2 emitted from these various regions. An SO_2 molecule emitted from the rest of world source region has a much greater potential to contribute to the burden of atmospheric sulfate than one emitted from, for example, Europe. This is due to a number of factors. A greater fraction of the SO_2 molecules originating from ROW is oxidized compared with other areas, and once formed, the aerosol has a longer residence time (that is, it is less readily scavenged, because it has been transported to regions where scavenging is less important). This statement can be quantified in terms of the sulfate potential. The ROW potential (or susceptibility) is a factor of four greater than that of Europe (which is the region with the lowest sulfate potential). The ROW region emissions are low compared to the other three source regions, but it generates burdens of comparable magnitude to that from the other source regions having much greater sulfur emissions.

Other differences between regions are also evident from the analysis. A substantially greater fraction of the sulfur dioxide emitted over Europe is oxidized to sulfate through the ozone pathway, than from any of the other regions. The large emissions in a limited area lead to larger concentrations of SO_2 than any other region. In this situation, there is not enough hydrogen peroxide to oxidize all the SO_2, and the importance of the O_3 reaction increases. These situations are encountered much less frequently in other areas of the world, where SO_2 concentrations are lower, and oxidant concentrations are higher.

The analysis suggests that there are also differences among the several source regions in the vertical distribution and horizontal extent of the propagation of the emissions. Near surface sulfate amounts generally originate from local source regions, but at higher altitudes the sulfate may originate from very distant sources. Sulfate from the Asian emissions reach the farthest from their point of origin. They make a noticable contribution to burdens in both hemispheres, primarily from plumes reaching out in the middle and upper troposphere. For example, perhaps 50% of the sulfate occuring on the west coast of the United States in summer originates from Asian emissions. Sulfate from the ROW sources remains trapped, primarily in the southern hemisphere. Similarly sulfate from North American and European emissions remains primarily in the northern hemisphere.

If these conclusions are robust, they suggests some caution be used in planning for future emissions in regions with a high aerosol potential. To zeroth order the burdens generated from these emission will have a corresponding effect on other climate factors (e.g. direct radiative forcing), although the strong sensitivity in aerosol optical properties to relative humidity means that aerosols near the surface may have a larger direct radiative effect than those located at higher altitudes. The situation is not so straightforward when one considers the possibility of the aerosols influencing the climate indirectly (either through changes to the clouds albedos, or to their microphysical properties). The indirect effects occur primarily in liquid phase clouds. If changes in the emissions result in changes to upper tropospheric aerosol amount, then this will have little influence on the drop size of liquid clouds, and thus little influence on cloud albedo or lifetime.

Acknowledgments.

We would like to thank Susan Solomon and Henning Rodhe for numerous discussions that helped clarify ideas discussed in this manuscript. We thank Brian Eaton for programming assistance. Work at BNL was supported by the Environmental Sciences Division of the U.S. Department of Energy and was performed under Contract No. DE-AC02-98CH10886.

References

Albrecht, B., 1989: Aerosols, cloud microphysics and fractional cloudiness. *Science*, **245**, 1227–1230.

Asselin, R., 1972: Frequency filter for time integrations. *Mon. Weather Rev.*, **100**, 487–490.

Barth, M., P. J. Rasch, J. T. Kiehl, C. M. Benkovitz and S. E. Schwartz, 1998: Sulfur chemistry in the NCAR CCM: Part I; Description, evaluation, features and influence of aqueous chemistry. *J. Geophys. Res.*, submitted.

Benkovitz, C., C. M. Berkowitz, R. C. Easter, S. Nemesure, R. Wagener and S. E. Schwartz, 1994: Sulfate over the North Atlantic and adjacent continental regions: Evaluation for October and November 1986 using a three-dimensional model driven by observation-derived meteorology. *J. Geophys. Res.*, **99**, 20725—20756.

Benkovitz, C., M. Scholtz, J. Pacyna, L. Tarrason, J. Dignon, E. Voldner, P. Spiro, J. Logan and T. Graedel, 1996: 1995 global gridded inventories of anthropogenic emissions of sulfur and nitrogen. *J. Geophys. Res.*, **101**, 29239—29254.

Bonan, G. B., 1996: *The NCAR Land Surface Model LSM version 1.0 coupled to the NCAR Community Climate Model*. NCAR Tech. Note, NCAR/TN–429+STR. Nat. Cent. for Atmos. Res., Boulder, Colo.

Charlson, R. J., S. E. Schwartz, J. M. Hales, R. D. Cess, J. A. C. Jr., J. E. Hansen and D. J. Hofmann, 1992: Climate forcing by anthropogenic aerosols. *Science*, **255**, 423—430.

Chin, M. and D. Jacob, 1996: Anthropogenic and natural contributions to tropospheric sulfate: A global model analysis. *J. Geophys. Res.*, in press.

Chin, M., D. J. Jacob, G. M. Gardner, M. Foreman-Fowler, P. A. Spiro and D. L. Savoie, 1996: A global three dimensional model of tropospheric sulfate. *J. Geophys. Res.*, pp. 18667—18690.

Chuang, C. C., J. E. Penner, K. E. Taylor, A. S. Grossman and J. J. Walton, 1997: An assessment of the radiative effects of anthropogenic sulfate. *J. Geophys. Res.*, **102**, 3761–3778.

Feichter, J., E. Kjellström, H. Rodhe, F. Dentener, J. Lelieveld and G.-J. Roelofs, 1996: Simulation of the tropospheric sulfur cycle in a global climate model. *Atmos. Environ.*, **30**(10), 1693–1707.

Feichter, J., U. Lohmann and I. Schult, 1997: The atmospheric sulfur cycle and its impact on the shortwave radiation. *Clim. Dyn.*, **13**, 235—256.

Graf, H.-F., J. Feichter and B. Langmann, 1997: Volcanic sulfur emissions: Estimates of source strength and its contribution to the global sulfate distribution. *J. Geophys. Res.*, **102**, 10727—10738.

Hartley, D., D. Williamson, P. Rasch and R. Prinn, 1994: Examination of tracer transport in the NCAR CCM2 by comparison of $CFCl_3$ simulations with ALE/GAGE observations. *J. Geophys. Res.*, **99**, 12,855–12,896.

Kasibhatla, P., W. L. Chameides and J. St. John, 1997: A three-dimensional global model investigation of seasonal variations in the atmospheric burden of anthropogenic sulfate aerosols. *J. Geophys. Res.*, **102**, 3737–3760.

Kent, G. S., M. P. McCormick and P.-H. Wang, 1994: Validation of stratospheric aerosol and gas experiments. *J. Geophys. Res.*, **99**, 10333—10339.

Kiehl, J. T., J. Hack, G. B. Bonan, B. A. Boville, B. P. Briegleb, D. L. Williamson and P. J. Rasch, 1996: *Description of the NCAR Community Climate Model (CCM3)*. NCAR Tech. Note, NCAR/TN–420+STR. Nat. Cent. for Atmos. Res., Boulder, Colo.

Kiehl, J. T., T. L. Schneider, P. J. Rasch, M. Barth and J. Wong, 1998: Radiative forcing due to sulfate aerosols from simulations with the NCAR Community Climate Model (CCM3). *J. Geophys. Res.*, submitted.

Langner, J. and H. Rodhe, 1991: A global three-dimensional model of the tropospheric sulfur cycle. *J. Atmos. Chem.*, **13**, 225—263.

Langner, J., H. Rodhe, P. J. Crutzen and P. Zimmermann, 1992: Anthropegenic influence on the distribution of tropospheric sulphate aerosol. *Nature*, **359**, 712—715.

Lelieveld, J., G.-J. Roelofs, L. Ganzeveld, J. Feichter and H. Rodhe, 1997: Terrestrial sources and distribution of atmospheric sulphur. *Phil. Trans. R. Soc. Lond.*, **352**, 149–158.

Müller, J.-F. and G. P. Brasseur, 1995: IMAGES: A three-dimensional chemical transport model of the global troposphere. *J. Geophys. Res.*, **100**, 16445—16490.

Pham, M., J.-F. Müller, G. Brasseur, C. Granier and G. Megie, 1995: A three-dimensional study of the tropospheric sulfur cycle. *J. Geophys. Res.*, **100**, 26061—26092.

Randall, D. A., Ed., 1998: *Special issue of J. Clim.devoted to the Climate Systems Model*. Vol. 11. Americam Meteorological Society.

Rasch, P. J., J. Feichter, K. Law, N. Mahowald, J. Penner, C. Benkovitz, C. Genthon, C. Giannakopoulos, P. Kasibhatla, D. Koch, H. Levy, T. Maki, M. Prather, D. L. Roberts, G.-J. Roelofs, D. Stevenson, Z. Stockwell, S. Taguchi, M. Kritz, M. Chipperfield, D. Baldocchi, P. McMurry, L. Barrie, T. Balkanski, R. Chatfield, E. Kjellstrom, M. Lawrence, H. N. Lee, J. Lelieveld, K. J. Noone, J. Seinfeld, G. Stenchikov, S. Schwarz, C. Walcek and D. Williamson, 1998: An assessment of scavenging and deposition processes in global models; results from the WCRP Cambridge workshop of 1995. *Tellus*, submitted.

Rasch, P. J. and J. E. Kristjánsson, 1998: A comparison of the CCM3 model climate using diagnosed and predicted condensate parameterizations. *J. Clim.*, **11**, 1587—1614.

Roelofs, G.-J., J. Lelieveld and L. Ganzeveld, 1998: Simulation of global sulfate distribution and the influence on effective cloud drop radii with a coupled photochemistry-sulfur cycle model. *Tellus*, **50B**, 224–242.

Turco, R. P., R. C. Whitten and O. B. Toon, 1982: Stratospheric aerosols: obvservations and theory. *Revs. Geophys. Space Phys.*, **20**, 233—279.

Twomey, S. A., 1974: Pollution and the planetary albedo. *Atmos. Environ.*, **8**, 1251–1256.

Waugh, D. W., T. M. Hall, W. J. Randel, P. J. Rasch, B. A. Boville, K. A. Boering, S. C. Wofsy, D. C. Daube, J. W. Elkins, D. W. Fahey, G. S. Dutton, C. M. Volk and P. F. Vohralik, 1997: Three-dimensional simulations of long-lived tracers using winds from MACCM2. *J. Geophys. Res.*, **102**, 21493–21513.

Wojcik, G. S. and J. S. Chang, 1997: A re-evaluation of sulfur budgets, lifetimes and scavenging ratios for eastern north america. *J. Atmos. Chem.*, **26**, 109—145.

This preprint was prepared with AGU's LaTeX macros v4, with the extension package 'AGU^{++}' by P. W. Daly, version 1.5e from 1997/11/18.